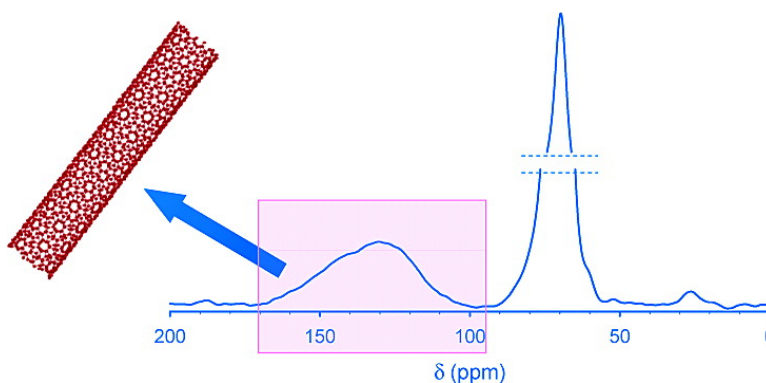


## NMR Detection of Single-Walled Carbon Nanotubes in Solution

Alex Kitaygorodskiy, Wei Wang, Su-Yuan Xie, Yi Lin, K. A. Shiral  
 Fernando, Xin Wang, Liangwei Qu, Bailin Chen, and Ya-Ping Sun

*J. Am. Chem. Soc.*, **2005**, 127 (20), 7517-7520 • DOI: 10.1021/ja050342a • Publication Date (Web): 29 April 2005

Downloaded from <http://pubs.acs.org> on March 25, 2009



### More About This Article

Additional resources and features associated with this article are available within the HTML version:

- Supporting Information
- Links to the 13 articles that cite this article, as of the time of this article download
- Access to high resolution figures
- Links to articles and content related to this article
- Copyright permission to reproduce figures and/or text from this article

[View the Full Text HTML](#)



**ACS Publications**  
 High quality. High impact.

## NMR Detection of Single-Walled Carbon Nanotubes in Solution

Alex Kitaygorodskiy, Wei Wang, Su-Yuan Xie, Yi Lin, K. A. Shiral Fernando, Xin Wang, Liangwei Qu, Bailin Chen, and Ya-Ping Sun\*

Contribution from the Department of Chemistry and Laboratory for Emerging Materials and Technology, Clemson University, Clemson, South Carolina 29634-0973

Received January 18, 2005; E-mail: syaping@clemson.edu

**Abstract:** The detection of nanotube carbons in solution by  $^{13}\text{C}$  NMR is reported. The highly soluble sample was from the functionalization of  $^{13}\text{C}$ -enriched single-walled carbon nanotubes (SWNTs) with diamine-terminated oligomeric poly(ethylene glycol) (PEG<sub>1500N</sub>). The ferromagnetic impurities due to the residual metal catalysts were removed from the sample via repeated magnetic separation. The nanotube carbon signals are broad but partially resolved into two overlapping peaks, which are tentatively assigned to nanotube carbons on semiconducting (upfield) and metallic (downfield) SWNTs. The solid-state NMR signals of the same sample are similarly resolved. Mechanistic and practical implications of the results are discussed.

### Introduction

There have been extensive recent investigations on the functionalization of single-walled carbon nanotubes (SWNTs).<sup>1–3</sup> The functionalization typically renders solubilities of the nanotubes, enabling their characterization in homogeneous organic and/or aqueous solutions. NMR is obviously one of the most desirable instrumental methods for studying the structures and properties of functionalized carbon nanotubes. However, a number of technical difficulties have probably hindered a direct  $^{13}\text{C}$  NMR probing of the functionalized nanotube itself in solution, such as limited sample solubility and the presence of ferromagnetic impurities, among others. Thus, the available solution-phase NMR results are centered on the characterization of the functional groups. For example, Chen et al. reported the use of  $^1\text{H}$  NMR results to validate their proposed noncovalent  $\pi$ -stacking mechanism for the functionalization of SWNTs with poly(arylene ethynylene) polymers.<sup>4</sup> Holzinger et al. used  $^1\text{H}$  NMR to characterize their soluble SWNT samples functionalized by various substituted oxycarbonyl nitrene compounds.<sup>5a</sup> The NMR signals from the functional groups on SWNTs are often broader than those from the free functionalization agent, with generally similar patterns but sometimes shifting to the upfield.<sup>4,5</sup>

Solid-state  $^{13}\text{C}$  NMR has been applied to the characterization of nanotube carbons in the functionalized SWNT samples.<sup>6,7</sup>

The signals of the nanotube  $\text{sp}^2$  carbons are generally broad, centered around 120–130 ppm, similar to those for unfunctionalized SWNTs.<sup>8–11</sup> In a recent study of polymer-functionalized SWNTs, solid-state 2D  $^1\text{H}$ – $^{13}\text{C}$  heteronuclear correlation spectroscopy was employed for evidence on significant interactions of the functional groups with the nanotube.<sup>7</sup> Even for solid-state NMR, however, it is widely acknowledged that NMR measurements and results can be negatively affected by the presence of substantial ferromagnetic impurities from the residual metal catalysts used in the nanotube production.<sup>6–10</sup> Despite the development of various purification methods,<sup>12</sup> the catalyst residues can often survive some of the rather harsh chemical and thermal treatments of carbon nanotube samples. As a result, SWNTs produced by using catalysts of nonferromagnetic metals (Rh/Pd or Pt/Rh, for example) have been used in some recent NMR studies.<sup>8,11</sup>

Here, we report results from the first attempt of a solution-phase  $^{13}\text{C}$  NMR study of nanotube carbons in functionalized SWNTs. The nanotube sample was produced with  $^{13}\text{C}$  isotope enrichment. The high nanotube equivalent solubility was

- (1) (a) Chen, J.; Hamon, M. A.; Hu, H.; Chen, Y.; Rao, A. M.; Eklund, P. C.; Haddon, R. C. *Science* **1998**, *282*, 95–98. (b) Niyogi, S.; Hamon, M. A.; Hu, H.; Zhao, B.; Bhowmik, P.; Sen, R.; Itkis, M. E.; Haddon, R. C. *Acc. Chem. Res.* **2002**, *35*, 1105–1113.
- (2) (a) Sun, Y.-P.; Fu, K.; Lin, Y.; Huang, W. *Acc. Chem. Res.* **2002**, *35*, 1096–1104. (b) Lin, Y.; Taylor, S.; Li, H.; Fernando, K. A. S.; Qu, L.; Wang, W.; Gu, L.; Zhou, B.; Sun, Y.-P. *J. Mater. Chem.* **2004**, *14*, 527–541.
- (3) (a) Hirsch, A. *Angew. Chem., Int. Ed.* **2002**, *41*, 1853–1859. (b) Bahr, J. L.; Tour, J. M. *J. Mater. Chem.* **2002**, *12*, 1952–1958.
- (4) Chen, J.; Liu, H.; Weimer, W. A.; Halls, M. D.; Waldeck, D. H.; Walker, G. C. *J. Am. Chem. Soc.* **2002**, *124*, 9034–9035.
- (5) (a) Holzinger, M.; Abraham, J.; Whelan, P.; Graupner, R.; Ley, L.; Hennrich, F.; Kappes, M.; Hirsch, A. *J. Am. Chem. Soc.* **2003**, *125*, 8566–8580. (b) Ruther, M. G.; Frehill, F.; O'Brien, J. E.; Minett, A. I.; Blau, W. J.; Vos, J. G.; in het Panhuis, M. *J. Phys. Chem. B* **2004**, *108*, 9665–9668.

- (6) Peng, H.; Alemany, L. B.; Margrave, J. L.; Khabashesku, V. N. *J. Am. Chem. Soc.* **2003**, *125*, 15174–15182.
- (7) Cahill, L. S.; Yao, Z.; Adronov, A.; Penner, J.; Moonosawmy, K. R.; Kruse, P.; Goward, G. R. *J. Phys. Chem. B* **2004**, *108*, 11412–11418.
- (8) Tang, X.-P.; Kleinhammes, A.; Shimoda, H.; Fleming, L.; Bennoune, K. Y.; Sinha, S.; Bower, C.; Zhou, O.; Wu, Y. *Science* **2000**, *288*, 492–494.
- (9) (a) Goze-Bac, C.; Latil, S.; Lauginie, P.; Jourdain, V.; Conard, J.; Duclaux, L.; Rubio, A.; Bernier, P. *Carbon* **2002**, *40*, 1825–1842. (b) Latil, S.; Henrard, L.; Goze Bac, C.; Bernier, P.; Rubio, A. *Phys. Rev. Lett.* **2001**, *86*, 3160–3163.
- (10) Hayashi, S.; Hoshi, F.; Ishikura, T.; Yumura, M.; Ohshima, S. *Carbon* **2003**, *41*, 3047–3056.
- (11) (a) Kleinhammes, A.; Mao, S.-H.; Yang, X.-J.; Tang, X.-P.; Shimoda, H.; Lu, J. P.; Zhou, O.; Wu, Y. *Phys. Rev. B* **2003**, *68*, 075418. (b) Goze-Bac, C.; Bernier, P.; Latil, S.; Jourdain, V.; Rubio, A.; Jhang, S. H.; Lee, S. W.; Park, Y. W.; Holzinger, M.; Hirsch, A. *Curr. Appl. Phys.* **2001**, *1*, 149–155. (c) Goze-Bac, C.; Latil, S.; Vaccarini, L.; Bernier, P.; Gaveau, P.; Tahir, S.; Micholet, V.; Aznar, R.; Rubio, A.; Meternier, K.; Beguin, F. *Phys. Rev. B* **2001**, *63*, 100302.
- (12) Haddon, R. C.; Sippel, J.; Rinzler, A. G.; Papadimitrakopoulos, F. *MRS Bull.* **2004**, *29*, 252–259.

achieved via the known functionalization of SWNTs with diamine-terminated oligomeric poly(ethylene glycol). The ferromagnetic impurities due to the residual metal catalysts were effectively removed from the functionalized nanotube sample in solution via repeated magnetic separation. The solution-phase NMR results are compared with those from solid-state NMR measurements. The partially resolved nanotube carbon signals in the NMR spectra are discussed in terms of theoretically predicted difference in chemical shifts between semiconducting and metallic SWNTs.<sup>9</sup>

## Experimental Section

**Materials.** Amorphous <sup>13</sup>C powder (99.99% carbon, <sup>13</sup>C content >98%) and graphite powder (CVP grade) were supplied by Icon Isotopes and Bay Carbon, respectively. Carbon cement was obtained from Dylon Industries. Powdery Ni (2.2–3.0 μm, 99.9%) and Co (1–6 μm, 99.8%) were purchased from Alfa Aesa. *O,O'*-Bis(3-aminopropyl) poly(ethylene glycol) of average molecular weight,  $M_w \sim 1500$  (PEG<sub>1500N</sub>), and KCl (>99%) were obtained from Aldrich and deuterated solvents from Cambridge Isotope Laboratories. Cellulose ester dialysis tubing with a molecular weight cutoff (MWCO) of 12 000 was supplied by Sigma.

The SWNT sample without <sup>13</sup>C enrichment was purchased from Carbon Solutions. For the purification, raw material (1.2 g) was heated in air at 300 °C for 30 min, followed by refluxing in HNO<sub>3</sub> (2.6 M, 500 mL) for 24 h. The mixture was then cooled to room temperature and subject to centrifugation (~1400g, Fisher Scientific Centrifuge 228 Centrifuge). The sediment was repeatedly washed with deionized water and dried under vacuum to yield a purified SWNT sample (336 mg).

**Measurements.** Raman spectra were obtained on a Renishaw Raman spectrometer equipped with a 50 mW diode laser source for 785 nm excitation and a CCD detector. Thermogravimetric analysis (TGA) experiments were carried out on a Mettler Toledo TGA/SDTA851e system with a typical heating rate of 10 °C/min. Electron microscopy imaging was conducted on a Hitachi HD-2000 scanning transmission electron microscope (STEM) operated at 200 kV with digital imaging capability. The atomic absorption analysis service was provided by Goldie and Associates (Seneca, South Carolina). Samples for the analysis were digested by using hot HNO<sub>3</sub>/HCl-mixed acid in accordance with the EPA 200.2 method.

NMR measurements were performed on a Bruker Avance 500 NMR spectrometer equipped with a 4 mm magic angle spinning (MAS) probe-head for solids and a 5 mm auto-tune probe-head for solutions. For very broad signals, exponential multiplication with a line broadening up to 500 Hz was applied for each carbon FID (free induction decay), coupled with user-defined spline baseline correction in the data processing. The spin–lattice relaxation times of both solid and solution samples were measured with the inversion recovery pulse sequence. Since the solution and solid-state NMR experiments showed that the nanotube carbon signals were not affected by the proton decoupling, the reported NMR spectra were collected without the decoupling (to avoid overheating the sample and potential damage to the equipment in solid-state experiments).

**<sup>13</sup>C-Enriched SWNTs.** The laser ablation method<sup>13</sup> was used for the synthesis of <sup>13</sup>C-enriched SWNTs. The laser source was a Spectra Physics Quanta-Ray PRO-290 Q-switched Nd:YAG laser operated at 10 Hz (2 J/pulse at 1064 nm and 9 mm beam diameter). In a typical experiment, the ablation target was prepared by mixing powdery <sup>13</sup>C (0.80 g), graphite (1.52 g), Ni (0.236 g), and Co (0.236 g) with graphite cement (2.40 g) for hot-pressing (130 °C) into a pellet (about 10 mm thick and 18 mm in diameter), followed by baking at 180 °C for 5 h in air, curing at 810 °C for 8 h, and annealing at 1200 °C for 30 h in

argon flow (50 sccm, atmospheric pressure). The furnace temperature was set at 1150 °C, with a steady argon flow (62 sccm, 75 kPa), in the ablation experiment. The rubber-like carbon soot from the laser ablation was characterized by Raman, and the results were consistent with the expected substantial presence of <sup>13</sup>C-enriched SWNTs in the soot. According to the characteristic G-band shift, the atomic content of <sup>13</sup>C in the nanotubes was estimated as 16%.<sup>14</sup>

The purification of the <sup>13</sup>C-enriched SWNT sample was similar to that discussed above for the regular SWNT sample.

**Functionalization and Magnetic Separation.** In a typical experiment,<sup>15</sup> a purified <sup>13</sup>C-enriched SWNT sample (60 mg) was mixed with PEG<sub>1500N</sub> (1.2 g), and the mixture was heated to 120 °C. After 3 days at that temperature, the reaction mixture was cooled to ambient for repeated extraction with water. In each extraction, the soluble fraction containing the PEG<sub>1500N</sub>-functionalized nanotubes was separated from the insoluble residue via centrifuging at ~1400g for 15 min. Typically three repeats were performed, with the supernatant in the last repeat being colorless. The aqueous solutions from the repeated extractions were combined for magnetic separation.

The magnetic separation to remove residual metal catalysts in the solubilized sample was accomplished by using a commercially available magnetic separator (Dynal Biotech Model MPC-L).<sup>16</sup> Each separation experiment was for 2 days, and the experiment was repeated three times to ensure maximal precipitation of all magnetically responsive species. The final supernatant was recovered, followed by dialysis (MWCO ~ 12 000) against fresh deionized water for 3 days (removing free PEG<sub>1500N</sub>) to yield a colored aqueous solution of PEG<sub>1500N</sub>-functionalized <sup>13</sup>C-enriched SWNTs (PEG<sub>1500N</sub>-<sup>13</sup>C-SWNT).

The same procedure was applied to obtain a magnetically purified PEG<sub>1500N</sub>-functionalized SWNTs sample without <sup>13</sup>C enrichment for the nanotubes.

## Results and Discussion

The properties (appearance, solubility, nanotube content, <sup>1</sup>H NMR, microscopy images, etc.) of the PEG<sub>1500N</sub>-<sup>13</sup>C-SWNT sample are similar to those of their counterpart without <sup>13</sup>C enrichment already reported in the literature.<sup>15</sup> The high solubility of these functionalized nanotubes,<sup>15</sup> coupled with the <sup>13</sup>C enrichment, made it possible to probe nanotube carbons in solution-phase NMR measurements. As shown in Figure 1 for PEG<sub>1500N</sub>-<sup>13</sup>C-SWNT in D<sub>2</sub>O (solution concentration ~ 36 mg/mL SWNT equivalent), the nanotube sp<sup>2</sup> carbons exhibit a broad signal centered at ~132 ppm (fwhm ~ 28 ppm), which is consistent with theoretical predictions<sup>17</sup> and close to those observed in solid-state NMR.<sup>6,7</sup> Obviously, nanotube carbons can be detected by NMR in solution.

The broadness in the signals reflects the chemical shift dispersion of nanotube carbons, which are likely inhomogeneous due to different nanotube chiralities, lengths, adjacent defects, etc.<sup>9,17</sup> Interestingly, however, there are some distinctive features in the broad signals, which through deconvolution (resolving the curve into underlying peaks) can be represented by two Lorentzian peaks of similar line-widths (~20 ppm, Figure 1). The ratio of area under the peak centered at 128 ppm to that at 144 ppm is ~1.8. A variation of relaxation delay time from 3 to 0.4 s had little effect on the signal shape, with similar line-widths and chemical shifts. We tentatively assign the two peaks

(14) Liu, L.; Fan, S. *J. Am. Chem. Soc.* **2001**, *123*, 11502–11503.

(15) (a) Huang, W.; Fernando, S.; Allard, L. F.; Sun, Y.-P. *Nano Lett.* **2003**, *3*, 565–568. (b) Fernando, K. A. S.; Lin, Y.; Sun, Y.-P. *Langmuir* **2004**, *20*, 4777–4778.

(16) Pyle, B. H.; Broadway, S. C.; McFeters, G. A. *Appl. Environ. Microbiol.* **1999**, *65*, 1966–1972.

(17) Zurek, E.; Autschbach, J. *J. Am. Chem. Soc.* **2004**, *126*, 13079–13088.

(13) Thess, A.; Lee, R.; Nikolaev, P.; Dai, H.; Petit, P.; Robert, J.; Xu, C.; Lee, Y. H.; Kim, S. G.; Rinzler, A. G.; Colbert, D. T.; Scuseria, G. E.; Tomanek, D.; Fisher, J. E.; Smalley, R. E. *Science* **1996**, *273*, 483–487.

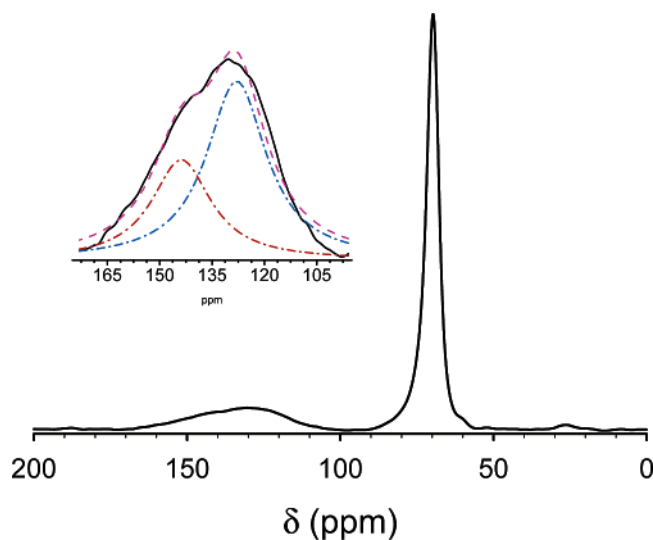


**Figure 1.** The  $^{13}\text{C}$  NMR spectrum of  $\text{PEG}_{1500\text{N}}\text{-}^{13}\text{C}\text{-SWNT}$  in  $\text{D}_2\text{O}$  solution (31 000  $45^\circ$  scans, 2 s relaxation delay, acquired in the CP-MAS probe but without spinning and decoupling). Shown in the inset is a deconvolution based on two Lorentzian peaks (reproduced curve, - - -). The 70 ppm signal is due to nanotube-attached PEG functional groups.

to semiconducting (upfield) and metallic (downfield) SWNTs.<sup>18</sup> In fact, the observed difference in their chemical shifts ( $\sim 16$  ppm) is in reasonable agreement with what has been predicted by recent theoretical calculations.<sup>9</sup> These calculations suggested that there should be an approximately  $\sim 12$  ppm upfield shift for the semiconducting nanotube carbons from their metallic counterparts due to the localized ring currents.<sup>9</sup>

There was also suggestion that the broad solid-state NMR signals of nanotube carbons could be deconvoluted into two peaks corresponding to semiconducting and metallic SWNTs, despite the fact that those signals were not resolved at all.<sup>9a</sup> The peak shoulder structure shown in Figure 1 represents the first experimental confirmation that there is indeed a pair of broad signals associated with the  $\text{sp}^2$  carbons in SWNTs. The acquisition of the partially resolved  $^{13}\text{C}$  NMR benefited significantly from the effective removal of residual metal catalysts via repeated magnetic precipitation in solution. It is well-known that the ferromagnetic residues associated with the Ni-Co catalysts interfere with NMR measurements.<sup>8</sup> These residues are often encapsulated in carbon cages or structural cavities and are, thus, impossible to remove completely in the chemical purification.<sup>12,21</sup> The solubilization of the nanotube sample enabled the solution-phase magnetic separation. The separation was effective, as confirmed by STEM analyses of the separated samples (Figure 2) and by TGA analysis (negligible residue), and also was reflected in the NMR results (diminished spinning sidebands in the solid-state NMR spectrum, for example). According to the atomic absorption analysis

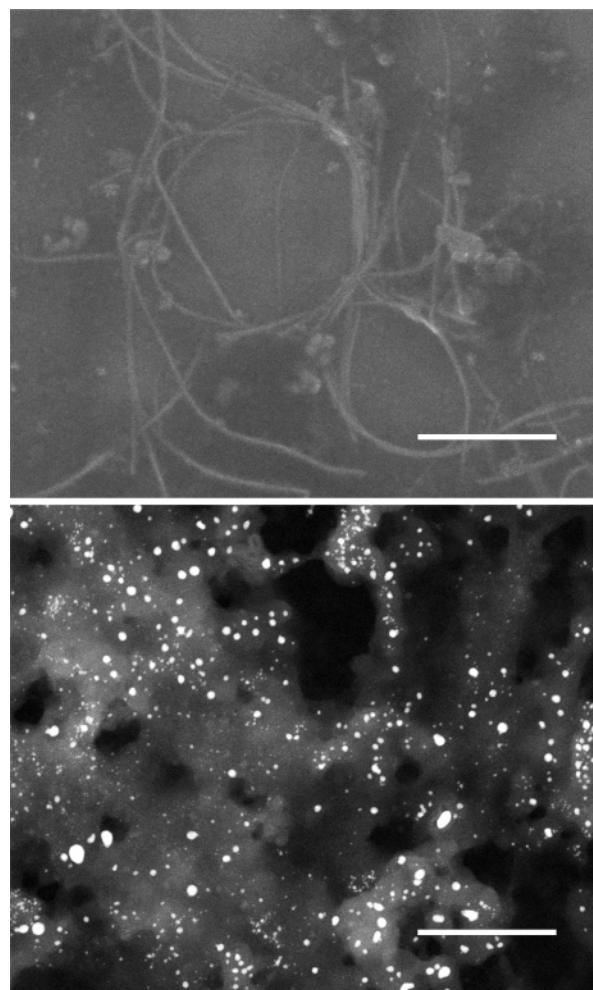


**Figure 2.** STEM images of the  $\text{PEG}_{1500\text{N}}\text{-}^{13}\text{C}\text{-SWNT}$  sample (in secondary electron mode, top) and the precipitate from magnetic separation (in Z-contrast mode, bottom). The Z-contrast imaging of the  $\text{PEG}_{1500\text{N}}\text{-}^{13}\text{C}\text{-SWNT}$  sample revealed no metals. Scale bars = 300 nm.

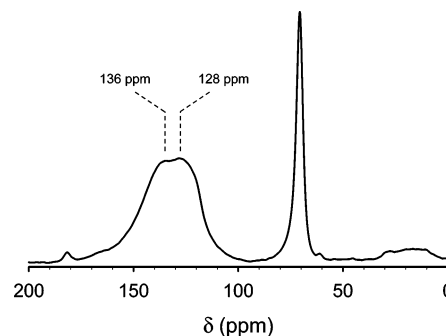


**Figure 3.** The solid-state MAS  $^{13}\text{C}$  NMR spectrum of  $\text{PEG}_{1500\text{N}}\text{-}^{13}\text{C}\text{-SWNT}$  (in a mixture with KCl, 11 000  $90^\circ$  scans, 2 s relaxation delay, 14 kHz spinning rate, single pulse sequence, no decoupling).

of the  $\text{PEG}_{1500\text{N}}\text{-}^{13}\text{C}\text{-SWNT}$  sample, the Ni content was  $<0.067$  wt % and the Co content was much lower (below the detection limit).

The solid-state  $^{13}\text{C}$  MAS NMR spectrum of the  $\text{PEG}_{1500\text{N}}\text{-}^{13}\text{C}\text{-SWNT}$  sample was acquired for comparison with the solution-phase result. The nanotube carbon signals in the solid-state spectrum are equally broad, with two obvious overlapping peaks at  $\sim 128$  and  $\sim 136$  ppm (Figure 3). Similar to the solution-phase signals, these two peaks may also be assigned to semiconducting and metallic SWNTs. The relative intensities

- (18) The functionalization may be attributed to ionic bonds between the amino groups on  $\text{PEG}_{1500\text{N}}$  and nanotube-bound carboxylic acids,<sup>15,19</sup> and also to the adsorption of amino moieties onto the nanotube surface.<sup>20</sup> It seems difficult to expect that there could be enough difference in the functional group coverage on the nanotube surface to result in the partially resolved peaks in nanotube carbon signals. Nevertheless, it remains a possible alternative in the explanation of these signals.
- (19) Chen, J.; Rao, A. M.; Lyuksyutov, S.; Itkis, M. E.; Hamon, M. A.; Hu, H.; Cohn, R. W.; Eklund, P. W.; Colbert, D. T.; Smalley, R. E.; Haddon, R. C. *J. Phys. Chem. B* **2001**, *105*, 2525–2528.
- (20) Chattopadhyay, D.; Galeska, I.; Papadimitrakopoulos, F. *J. Am. Chem. Soc.* **2003**, *125*, 3370–3375.
- (21) Thiên-Nga, L.; Hernadi, K.; Ljubović, E.; Garaj, S.; Forró, L. *Nano Lett.* **2002**, *2*, 1349–1352.

of the two peaks are somewhat different in solid state versus in solution. Additionally, the overall intensity of the nanotube carbon signals in reference to that of PEG<sub>1500N</sub> functional groups is significantly higher in solid state than in solution. These two differences between solid-state and solution-phase NMR results may share the same cause. As in other soluble functionalized SWNTs, the PEG<sub>1500N</sub>-<sup>13</sup>C-SWNT sample contains bundled nanotubes in solution. The tumbling of larger bundles may proceed too slow to eliminate such orientation-dependent contributions to the NMR line-width as chemical shift anisotropy and dipolar coupling. These species are essentially NMR "silent" in solution, corresponding to a lower effective nanotube carbon concentration to result in their relatively weaker overall signal intensity in the solution-phase NMR spectrum. The functionalized semiconducting SWNTs disperse better in solution, as made evident by recent experimental results.<sup>20</sup> Therefore, their NMR signals relative to those of their metallic counterparts are stronger in solution (Figure 1) than in the solid state (Figure 3).

There are apparently significant interactions between the nanotube carbons and the PEG moieties in the solid state, with the latter serving as spin-lattice relaxation centers. The relaxation time ( $T_1$ ) of the nanotube carbons was estimated by using the null-point approach based on the inversion recovery sequence.<sup>22</sup> Both nanotube components effectively "disappeared" at the same point,  $\tau_{\text{null}} \sim 0.16$  s, corresponding to  $T_1 \sim 0.2$  s. Despite the absence of ferromagnetic impurities in the PEG<sub>1500N</sub>-<sup>13</sup>C-SWNT sample, the estimated  $T_1$  is up to 2 orders of magnitude shorter than those of similarly <sup>13</sup>C-enriched SWNTs without functionalization.<sup>8,11a</sup> The interactions are also reflected in the NMR results of the PEG carbons. For PEG<sub>1500N</sub>-<sup>13</sup>C-SWNT in D<sub>2</sub>O solution, the spin-lattice relaxation time of PEG carbon signals (560 ms) is close to that in free PEG<sub>1500N</sub>

(710 ms). However, in solid state, the relaxation time of PEG carbons in the PEG<sub>1500N</sub>-<sup>13</sup>C-SWNT sample is more than an order of magnitude shorter (37 ms) than that in free PEG<sub>1500N</sub> (430 ms). It seems that the segmental mobility of PEG moieties in PEG<sub>1500N</sub>-<sup>13</sup>C-SWNT in the solid state is low, presumably with the motion of PEG carbons restricted by their proximity to the nanotubes. Such significant difference of the relaxation times for the nanotube-bound functional groups in solution phase versus in solid state is interesting. It may be exploited for potential applications in the NMR characterization of nanocomposite materials, such as probing interactions of carbon nanotubes with the polymeric matrix.

In summary, we demonstrated that the nanotube carbons in solution could readily be detected in <sup>13</sup>C NMR by using highly soluble functionalized SWNTs. The ferromagnetic impurities in the sample for NMR measurements were effectively removed via repeated magnetic separation. The nanotube carbon signals are broad, but partially resolved into two adjacent features, probably corresponding to nanotube carbons in semiconducting (upfield) and metallic (downfield) SWNTs. The solid-state NMR signals of the same sample are similarly resolved. These results suggest that <sup>13</sup>C NMR may be explored to serve as a useful tool in the characterization of SWNTs of different electronic structures.<sup>20,23</sup>

**Acknowledgment.** Financial support from NSF, NASA, and Center for Advanced Engineering Fibers and Films (NSF-ERC at Clemson University) is gratefully acknowledged.

**Supporting Information Available:** Raman spectra of <sup>13</sup>C-enriched SWNTs and SWNTs without enrichment. This material is available free of charge via the Internet at <http://pubs.acs.org>.

JA050342A

(22) Farrar, T. C.; Becker, E. D. *Pulse and Fourier Transform NMR*; Academic Press: New York, 1971.

(23) (a) Li, H.; Zhou, B.; Lin, Y.; Gu, L.; Wang, W.; Fernando, K. A. S.; Kumar, S.; Allard, L. F.; Sun, Y.-P. *J. Am. Chem. Soc.* **2004**, *126*, 1014–1015. (b) Fernando, K. A. S.; Lin, Y.; Wang, W.; Kumar, S.; Zhou, B.; Xie, S.-Y.; Cureton, L. T.; Sun, Y.-P. *J. Am. Chem. Soc.* **2004**, *126*, 10234–10235.